



Fortgeschrittenenpraktikum

Microwave Methods and Detection Techniques for Electron Spin Resonance

June 19, 2013

A. Bechtold and M. Suckert

1 Introduction

Electron spin resonance (ESR) originated more than sixty years ago, when Zavoisky (1945) reported the first successful measurement of ESR signals in several salts, copper sulfate and manganese sulfate [1]. ESR is applied whenever a system has unpaired electrons. For instance, it can be used to understand reactions involving free radicals in biology and chemistry or to study transition metal complexes in solids [2]. ESR has also been successfully used to study the electronic structure of defects in semiconductors [3]. More recently, the physics of spins, especially in semiconductors, received renewed interest in the framework of quantum computing, where spins are used as solid state-based quantum bits. In this context, ESR can be used to manipulate the qubits.

ESR requires the very controlled application and highly sensitive detection of microwaves. This can be achieved by so-called vector network analyzers (VNA). More generally, a VNA allows to characterize microwave devices, whole microwave circuits and the properties of materials at microwave frequencies. In this *Fortgeschrittenenpraktikum*, we will learn techniques to detect ESR using such a VNA. After an introduction to microwave theory and vector network analysis, we will characterize different microwave resonators using a VNA and study how the quality factor of a resonator influences the ESR signals. Moreover, to improve the detection efficiency of small signals the VNA is used to simulate a phase-sensitive lock-in amplifier leading to a highly sensitive signal detection technique.

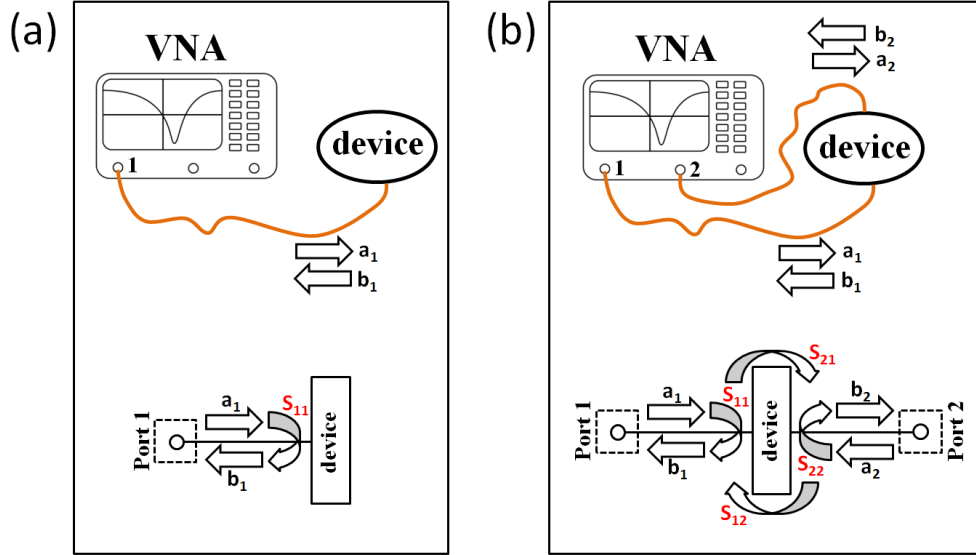


Figure 1: A two-port VNA has two operation modes to characterize a device under test. In the upper parts of the figure the wiring between the VNA and the device under test is shown, while in the lower parts block diagrams of the setup are depicted. (a) The ratio of reflected signal b_1 to incident signal a_1 using only one port (S_{11}) is measured. (b) Measurement of S_{11} , S_{12} , S_{21} and S_{22} using both ports.

2 What is vector network analysis?

A vector network analyzer has several ports on its front panel. On each port a microwave signal can be created and detected. We have to distinguish between waves $a_i = E_i \cos(\omega_i t + \varphi_i)$ emitted by the port i and waves $b_j = E_j \cos(\omega_j t + \varphi_j)$ impinging on port j . For the sake of simplicity consider the case that our VNA has only two ports on its front panel and a device under test (DUT) is connected to only one port while the other port is not used, as shown in Fig. 1(a). In this operation mode the reflection coefficient S_{11} is described as the ratio of the signal b_1 reflected by the DUT to the incident signal a_1

$$S_{11} = \frac{b_1}{a_1}.$$

Since the waves a_1 and b_1 have different phase relations with respect to each other, the reflection coefficient can be represented as a complex value. In contrast to a scalar network analyzer, the VNA is able to measure both, signal amplitude and phase relations.

Using two ports of the VNA, besides the reflection of the microwave at the DUT, the transmission through the DUT from one port to another port at the VNA can be measured. Figure 1(b) presents this second operation mode of the VNA measuring

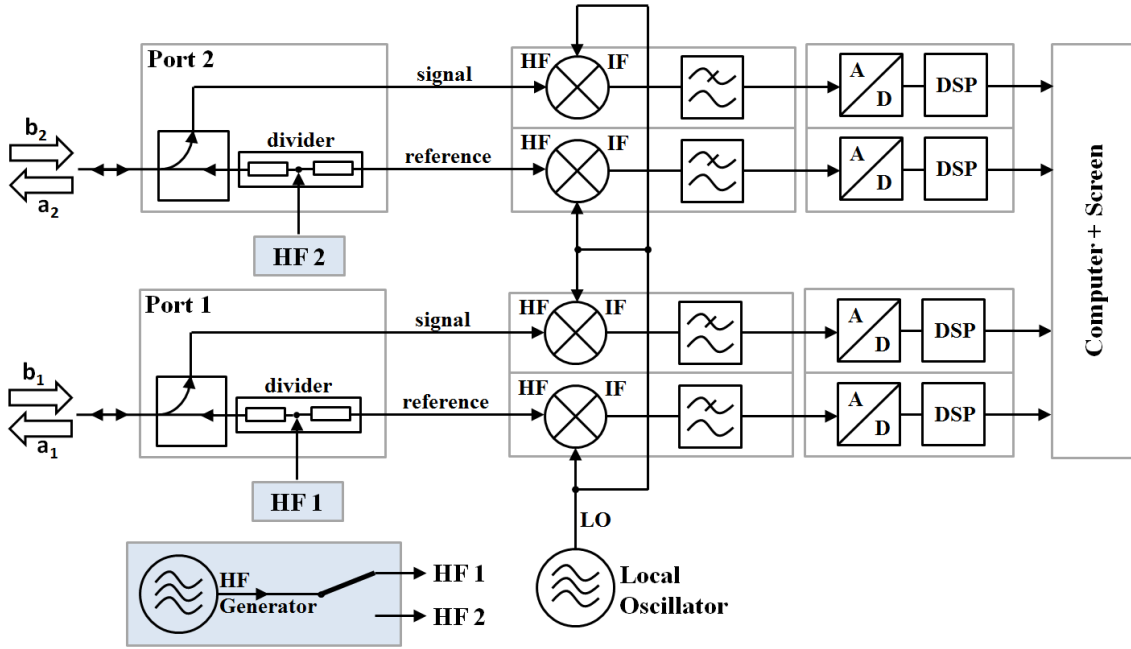


Figure 2: Simplified block diagram of a two-port VNA. For further details see text.

the complex transmission coefficients S_{12} and S_{21} . In this operation mode one port is configured such that only the incoming signal is detected and no signal is created at this port. To give an example: Measuring the transmission from port 1 to port 2, port 2 is configured such that $a_2 = 0$, resulting in the reflection and transmission coefficients

$$S_{11} = \left. \frac{b_1}{a_1} \right|_{a_2=0} \quad \text{and} \quad S_{21} = \left. \frac{b_2}{a_1} \right|_{a_2=0} .$$

The Working Principle of a Vector Network Analyzer

Figure 2 shows a simplified block diagram of a VNA. A high frequency (HF) signal generator with a widely tunable frequency range creates a sinusoidal wave which will be applied to one of the two ports. At the port the signal is divided into a reference signal and the signal provided to the actual port. In our notation this signal is signal a . A directive element separates the wave reflected from the DUT and impinging on the port from the wave emitted by the port. In the block diagram the reflected wave is labeled “signal” and corresponds to signal b while the signal labeled “reference” is proportional to signal a .

In a next step, both waves have to be digitized in order to process them with a Digital Signal Processor (DSP). A main restriction of an analog-to-digital converter (A/D) is its operation at comparatively low frequencies. Therefore, the high frequency

signal has to be down-converted. This step is carried out at the mixer stage where a signal with lower frequency created by a so-called local oscillator (LO) is mixed with signals a and b resulting in signals with an intermediate frequency (IF). Mixers are nonlinear components which can be approximated to first order in time domain as a signal multiplier. A multiplication of sinusoidal waves with frequencies f_{HF} and f_{LO} leads to an IF signal with the two frequency components

$$\begin{aligned} f_{\text{IF},1} &= f_{\text{HF}} - f_{\text{LO}} \quad \text{and} \\ f_{\text{IF},2} &= f_{\text{HF}} + f_{\text{LO}} \quad , \end{aligned}$$

which can be shown by application of the addition theorems. By this, we obtain signals consisting of a superposition of a low frequency oscillation and a high frequency oscillation. While the high frequency component can be attenuated using a low-pass filter, the low frequency part suitable for digitization can be processed in the DSP units. The DSP units extract physical values such as the S-parameters.

3 Theoretical Background of ESR

In this section, the fundamentals of ESR will be discussed. First, we focus on the interaction between the spin of an electron and an external magnetic field giving rise to the Zeeman splitting. The interaction strength is described by the g -factor. Due to spin-orbit coupling, the g -factor of paramagnetic states in a solid is modified with respect to the g -factor of the free electron g_e and depends strongly on the symmetry of the paramagnetic state. ESR can be excited when the energy of microwave radiation applied to the spin system matches the Zeeman energy. Using the Bloch equations, the relaxation of spin states and the shape of transition lines can be described.

3.1 An electron spin in a magnetic field: Zeeman interaction

The interaction between the magnetic moment originating from the electron spin $\hat{\mathbf{S}}$ and an external magnetic field \mathbf{B}_0 directed along \mathbf{z} is described by the Hamiltonian

$$\hat{\mathcal{H}} = g\mu_e\mathbf{B}_0 \cdot \hat{\mathbf{S}} \quad , \quad (1)$$

$$= g\mu_e B_0 \hat{S}_z \quad , \quad (2)$$

where $\mu_e = |e|\hbar/2m_e$ is the Bohr magneton, $|e|$ is the elementary charge, \hbar the reduced Planck's constant, m_e the free electron mass and g the electron g -factor.

For a system with effective spin $S = \frac{1}{2}$, the Hamiltonian (1) has two eigenvalues $E_{+1/2}$ and $E_{-1/2}$, which correspond to the $m_s = +1/2$ (spin up) and $m_s = -1/2$ (spin down)

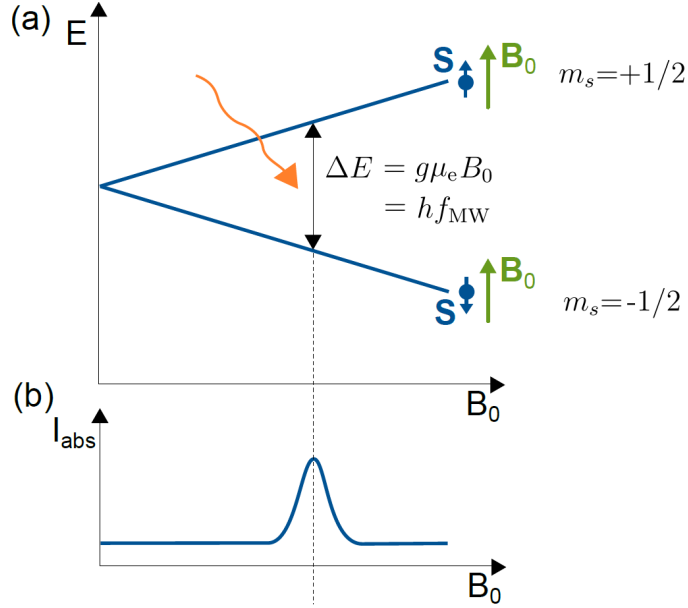


Figure 3: (a) Zeeman splitting of a system with $S=1/2$ as function of the applied external magnetic field B_0 . For each Zeeman branch the relative orientation of electron spin and B_0 is given. Additionally, the energy of the microwave radiation $E = hf_{\text{MW}}$ is shown. (b) Absorption signal I_{abs} of the spin system. If the microwave energy matches the energy difference between the two Zeeman levels, a maximum of absorption of microwave radiation is expected.

states, respectively. They depend linearly on the strength of the magnetic field B_0

$$E_{\pm 1/2} = \pm \frac{1}{2} g \mu_e B_0 . \quad (3)$$

Hence, upon application of an external magnetic field two eigenstates of the spin system are formed and separated by the Zeeman splitting, as shown in Fig. 3(a). The magnitude of this splitting is determined by the g -factor of the specific system, which for the case of the free electron is equal to $g_e = 2.0023193154 \pm 3.5 \times 10^{-9}$ [4].

In general, the g -factor of a spin system deviates from the free electron value g_e due to the spin-orbit interaction $\hat{\mathcal{H}}_{LS}$ [5], which is the interaction between the spin angular momentum $\hat{\mathbf{S}}$ and the magnetic moment of the orbital momentum $\hat{\mathbf{L}}$

$$\hat{\mathcal{H}}_{LS} = \lambda \hat{\mathbf{L}} \hat{\mathbf{S}} , \quad (4)$$

where λ quantifies the coupling strength between the two angular momenta. Although the orbital momentum of most molecules and ions in crystals is frequently quenched due to electrostatic interactions [6], there is always an effective residual angular momentum resulting from the admixture of the hypothetical “pure spin” ground state $|\Psi_0\rangle$ with certain excited states $|\Psi_n\rangle$ via the spin-orbit interaction.

This residual orbital angular momentum generates an effective local magnetic field that adds to the external field \mathbf{B}_0 , which results in a deviation of the g -factor from the free electron value

$$g_{ij} = g_e \delta_{ij} - 2\lambda \Lambda_{ij} , \quad (5)$$

where the matrix Λ_{ij} is given from second order perturbation theory by the expression [5, 7, 8]

$$\Lambda_{ij} = \sum_{n \neq 0} \frac{\langle \Psi_0 | \hat{L}_i | \Psi_n \rangle \langle \Psi_n | \hat{L}_j | \Psi_0 \rangle}{E_n - E_0} . \quad (6)$$

Here, \hat{L}_i is the i -component of the angular momentum operator, E_0 and E_n are the energies of the electronic ground and excited states, respectively. Note that according to the expression given in Eq. (5) the g -factor is described by a matrix, which means that in general this quantity is anisotropic and reflects the local symmetry of the system.

3.2 Resonance condition in ESR

In an ESR experiment, transitions are induced between the two Zeeman states using microwave radiation with the frequency f_{MW} as excitation. As can be seen in Fig. 3, resonant absorption occurs if the magnetic field is adjusted such that the radiation energy hf_{MW} is equal to the energy difference ΔE between the energy levels

$$hf_{\text{MW}} = \Delta E \equiv g\mu_e B . \quad (7)$$

The g -factor of the paramagnetic state is then obtained from the magnetic field at which the resonance is observed and the microwave used

$$g = \frac{hf_{\text{MW}}}{\mu_e B} . \quad (8)$$

In the general case, the selection rule for ESR transitions is

$$\Delta m_S = \pm 1 . \quad (9)$$

This restriction arises from momentum conservation as the microwave photon carries a spin $S=1$. For instance, in a spin system with $S=1$ only the transitions $m_S=-1 \leftrightarrow m_S=0$ and $m_S=0 \leftrightarrow m_S=+1$ are allowed in first order and transitions $m_S=-1 \leftrightarrow m_S=+1$ are “forbidden”.

A second restriction in terms of selection rules regards the orientation of the magnetic field component of the microwave field, which is labeled \mathbf{B}_1 -field. In order to induce spin transitions at resonance the \mathbf{B}_1 -field must be applied perpendicularly to the static magnetic field, the \mathbf{B}_0 -field. This will be come clearer in the classical description of ESR, which will be addressed in the next section.

3.3 Bloch equations

Until now, we restricted our discussion to the quantum mechanical description of the energy levels, between which the ESR transitions are induced. However, to describe the dynamics of ESR we have to focus on the time dependence of the total magnetization vector \mathbf{M} , which is a macroscopic quantity given by the sum over all individual magnetic momenta $\boldsymbol{\mu}_i$ in the ensemble,

$$\mathbf{M} = \frac{1}{V} \sum_i^N \boldsymbol{\mu}_i, \quad (10)$$

where V is the sample volume. A very useful description for the time dependence of \mathbf{M} was given by Bloch [9], which accounts for the relaxation processes occurring during an ESR experiment. This formalism was originally developed to explain the corresponding nuclear magnetic resonance (NMR) phenomena. However, it is also applicable in ESR to describe the time dependence of the magnetization vector \mathbf{M} when a spin system is subjected to a magnetic field \mathbf{B} comprising a static component B_0 , taken along \mathbf{z} without loss of generality, and an in-plane oscillating component B_1 perpendicular to \mathbf{z} . The time evolution of the magnetization \mathbf{M} is given by

$$\frac{d\mathbf{M}}{dt} = \gamma \mathbf{M} \times \mathbf{B} + \left. \frac{d\mathbf{M}}{dt} \right|_{\text{relax}}, \quad (11)$$

where $\gamma = g\mu_B/\hbar$ is the gyromagnetic ratio.

First, let's have a look at the relaxation part of the equation: If the magnetization \mathbf{M} is not in its thermal equilibrium state $\mathbf{M}_0 = M_0 \mathbf{z}$ the relaxation of the magnetization is described phenomenologically by the differential equation

$$\left. \frac{dM_z(t)}{dt} \right|_{\text{relax}} = -\frac{M_z(t) - M_0}{T_1}, \quad (12)$$

which assumes that \mathbf{M} relaxes exponentially towards \mathbf{M}_0 with a time constant T_1 . When this component of the magnetization relaxes to the equilibrium, the energy of the spin system is transferred to the lattice. Therefore, the characteristic time constant T_1 is called the spin-lattice relaxation time (or the longitudinal relaxation time).

For the transverse components of the magnetization \mathbf{M} the corresponding differential equations are

$$\left. \frac{dM_x}{dt} \right|_{\text{relax}} = -\frac{M_x(t)}{T_2} \quad \text{and} \quad (13)$$

$$\left. \frac{dM_y}{dt} \right|_{\text{relax}} = -\frac{M_y(t)}{T_2}, \quad (14)$$

where T_2 is the transverse or spin-spin relaxation time. In contrast to the spin-lattice relaxation, the spin-spin relaxation conserves the energy of the spin system.

The combination of Eqs. (11)-(14) results in the so-called Bloch equations,

$$\frac{dM_x}{dt} = \gamma(\mathbf{M} \times \mathbf{B})_x - \frac{M_x(t)}{T_2}, \quad (15)$$

$$\frac{dM_y}{dt} = \gamma(\mathbf{M} \times \mathbf{B})_y - \frac{M_y(t)}{T_2} \quad \text{and} \quad (16)$$

$$\frac{dM_z}{dt} = \gamma(\mathbf{M} \times \mathbf{B})_z - \frac{M_z(t) - M_0}{T_1}. \quad (17)$$

We now want to study the influence of the magnetic field \mathbf{B}_1 , which oscillates with the frequency $\omega = 2\pi f$. In the case of *slow adiabatic passage* [9], i.e. a fast relaxation and a low frequency of the oscillating magnetic field, the magnetization follows the field \mathbf{B}_1 . Solving the system of differential equations (15)-(17) for steady state conditions and taking into account that

$$\mathbf{M} = \chi \frac{\mathbf{B}}{\mu_m}, \quad (18)$$

where $\chi = \chi' + i\chi''$ is the dynamic susceptibility and μ_m is the permeability of the medium, the real and complex components of χ take the form [10, 11]

$$\chi' = \chi_0 \frac{\omega_0(\omega_0 - \omega)T_2^2}{1 + (\omega_0 - \omega)^2T_2^2 + \gamma^2B_1^2T_1T_2}, \quad (19)$$

$$\chi'' = \chi_0 \frac{\omega T_2}{1 + (\omega_0 - \omega)^2T_2^2 + \gamma^2B_1^2T_1T_2}. \quad (20)$$

Here, χ_0 is the static magnetic susceptibility and $\omega_0 = -\gamma B_0$. If B_1 is small (or rather $\gamma^2B_1^2T_1T_2 \ll 1$) Eqs. (19) and (20) simplify to

$$\chi' = (\omega_0 - \omega)T_2\chi'', \quad (21)$$

$$\chi'' = \chi_0 \frac{\omega_0 T_2}{1 + (\omega_0 - \omega)^2 T_2^2}. \quad (22)$$

χ' and χ'' are the *dispersive* and *absorptive* parts of the susceptibility, respectively, and are the quantities that can be measured in an ESR experiment. Equation (22) indicates that the absorption of an ideal spin ensemble has a Lorentzian line shape. In such a case, an analysis of the full-width-at-half-maximum determines the spin-spin relaxation time. Apart from the homogeneous broadening that is quantified through Eq. (22), an ESR line can also undergo an inhomogeneous broadening. Inhomogeneously broadened lines consist of a family of overlapping lines, which may result from unresolved line structure, e.g., caused by a distribution of g -factors or fluctuations of the magnetic field throughout the sample. The latter effects tend to produce lines which have a Gaussian line shape [2].

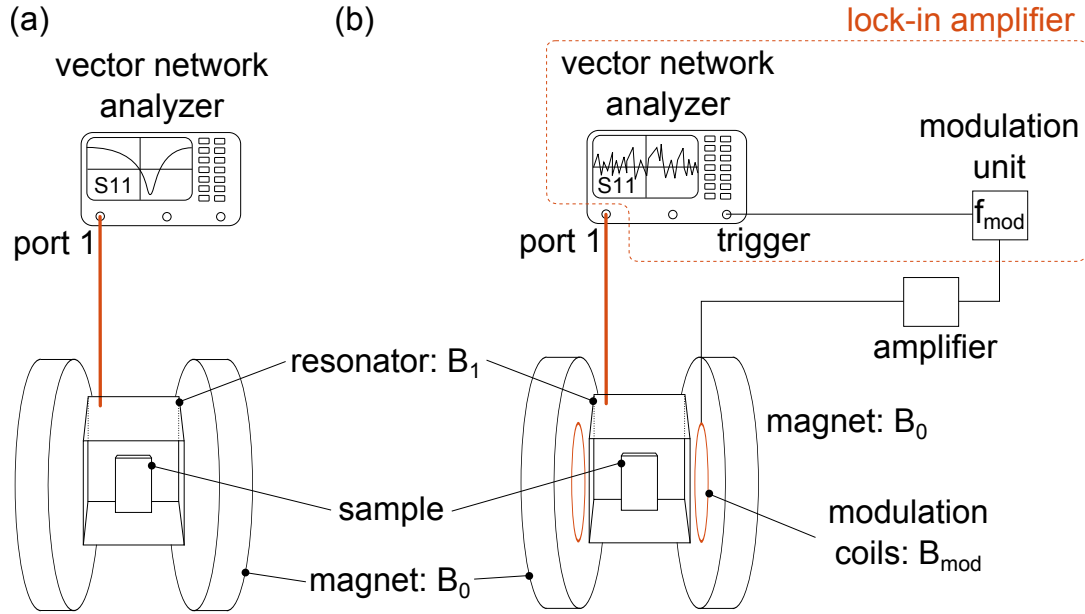


Figure 4: Experimental setup of ESR with microwave source and magnet. (a) The vector network analyzer applies a microwave and measures the reflected signal. (b) ESR spectroscopy using the phase-sensitive lock-in technique together with modulation coils allows to enhance the signal-to-noise ratio.

4 The Experimental Setup

In conventional ESR experiments, spin flip transitions are detected by monitoring the changes on the microwave radiation absorbed by the spin ensemble. Usually, continuous-wave ESR spectrometers operate at a constant microwave frequency f_{MW} with the magnetic field \mathbf{B}_0 varying linearly within the region of interest. In this laboratory experiment, we will study the fundamentals of magnetic resonance using continuous-wave ESR techniques with the help of a VNA as shown in Fig. 4.

In the following, a brief overview of the different parts of the experimental setup used in this laboratory experiment is given.

Magnetic field

As shown in the theoretical introduction, a magnetic field \mathbf{B}_0 is required to generate the Zeeman splitting. In this laboratory experiment, the external magnetic field is provided by two coils, as can be seen in Fig. 4(a). Since the microwave resonator (at the center of which the sample is placed) operates at a fixed frequency f_{res} , we need to vary the magnetic field in order to perform spectroscopy on an ESR absorption line. This is achieved by adjusting the current flowing through the coils. To determine

the g -factor, both, the microwave frequency and the resonant magnetic field have to be known. The microwave frequency can be read from the microwave source with high accuracy. In contrast, the magnetic field at the position of the sample has to be calibrated using a reference. One possibility is to determine the magnetic field by measuring a sample with a known g -factor, as it will be done in the experiment using DPPH (2,2-diphenyl-1-picrylhydrazyl).

Microwave source

In order to induce spin transitions, we use a VNA to create a microwave signal with known frequency and measure the signal reflected from a suitable device under test containing the sample to obtain the coefficient S_{11} , as described in Sec. 2. A common way to quantify the power of a microwave signal is using a logarithmic scale in units of decibel (dB)

$$L_{\text{dB}} = 10 \log_{10} \left(\frac{P_1}{P_0} \right)$$

where P_1 is the measured signal power and P_0 is a specified reference level. To give absolute values of power, the unit of dBm is used, where P_0 is 1 mW (e.g. 0 dBm = 1 mW, -20 dBm = 0.01 mW). The main advantage of such a logarithmically expressed quantity is that multiplying power ratios can be carried out just by simple addition and subtraction, which makes dealing with amplification and attenuation of signal amplitudes more comfortable.

Resonator

A resonator is used in this setup as DUT for two main reasons. First, a cavity resonator provides the possibility of separating the electric and magnetic fields of the microwave radiation since an electric field may affect the spin system adversely. Second, the resonator allows the enhancement of the magnetic field amplitude at the sample for the specific frequency ranges which it is designed for. This effect can be quantified by the quality factor Q , which is the ratio [12]

$$Q = 2\pi \frac{(\text{energy stored in the resonator})}{(\text{energy dissipated per cycle})} = \frac{f_{\text{res}}}{f_{\text{FWHM}}}. \quad (23)$$

Here, f_{res} is the resonance frequency of the cavity and f_{FWHM} is the full-width-at-half-maximum of the linear S_{11} spectrum of the cavity. A wide variety of resonators may be employed for measuring ESR. In this experiment, we use different types of resonators to study the difference between them:

- **RLC-Resonator:** The easiest and most instructive way to design a resonator is to connect an inductive coil and a capacitor in series as depicted in Fig. 5(a), the so-called RLC-resonator [13], where the resistive contribution comes from

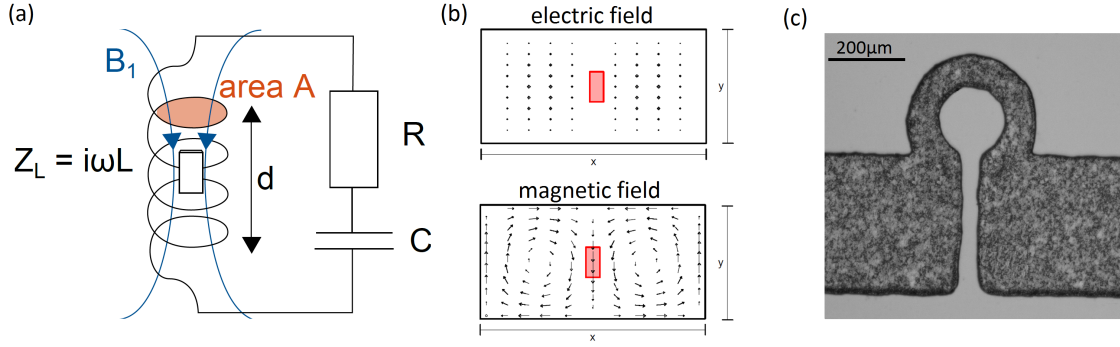


Figure 5: Different types of resonators. (a) RLC-resonator. (b) Electric and magnetic field components in a rectangular TE_{102} cavity resonator shown in cross section. The red box marks the area of good separation of fields where the sample is placed. (c) Image of a microstrip resonator. The geometry of stripline width, gap and ring determine the resonance frequency of the resonator.

the electric cable. The inductance of a long and thin coil with N loops, length l and cross section A containing a sample inside is given by

$$L = \mu_0 \left[1 + (\chi' + i\chi'') \frac{V_{\text{sample}}}{V_{\text{coil}}} \right] \frac{AN^2}{l}. \quad (24)$$

Here, V_{sample} is the volume of the sample, V_{coil} is the internal volume of the coil and $q = V_{\text{sample}}/V_{\text{coil}}$ is called the filling factor. When a resonator is tuned, at its resonance frequency

$$f_{\text{res}} = \frac{1}{2\pi\sqrt{LC}} \quad (25)$$

the complex impedance becomes zero. Under ESR condition, the impedance of the resonator changes via a change in $\chi = \chi' + i\chi''$. This change leads to a small change in the resonance frequency of the resonator and its quality factor Q , which can be detected by analyzing the S_{11} -spectrum of the resonator.

- **Cavity Resonator:** The most common type of resonators in ESR spectroscopy are resonant cavities, often of rectangular shape. A cavity resonator is a hollow conducting box with the geometry designed to obtain a standing microwave within the box as shown in Fig. 5(b). The figure shows the separation of magnetic and electric components of the microwave. Our resonator has been designed to operate at X-band frequencies around $f_{\text{res}} = 9.2$ GHz. By tuning the cavity geometry, e.g. by adjusting a screw at the cavity, it is possible to tune the resonance frequency of the cavity.
- **Microstrip Resonator:** Today, resonators made of microstrip lines are increasingly used instead of cavity resonators [14]. Such microstrip resonators, as depicted in Fig. 5(c), are cheap to fabricate and allow the application of

high frequencies (up to $f_{res} = 20$ GHz and more) with high quality and filling factors.

Depending on the quality factor of a resonator, the detected ESR signal is hardly sufficient in intensity to observe a change in the dynamic susceptibility. However, the detection sensitivity can be greatly improved using a lock-in method.

Lock-in amplifier (modulation coils + VNA)

The lock-in technique provides the possibility to detect small signal amplitudes with frequency $\omega_{mod} = 2\pi f_{mod}$ even in the presence of strong noise. This advantage makes the lock-in technique an important part of this *Fortgeschrittenenpraktikum*.

A simple way to selectively filter out a signal is to apply a Fourier transformation. The real coefficients which represent the amplitudes of the signal in-phase and out-of-phase relative to a reference signal are given by

$$a_{\omega_{mod}} = \frac{2}{T} \int_{-T/2}^{T/2} g(t) \cos(\omega_{mod}t) dt \quad \text{and} \quad (26)$$

$$b_{\omega_{mod}} = \frac{2}{T} \int_{-T/2}^{T/2} g(t) \sin(\omega_{mod}t) dt . \quad (27)$$

Here, $g(t) = g(t + T)$ is an arbitrary periodic function with the periodicity T . The fact, that $\sin(\omega_{mod}t)$ and $\cos(\omega_{mod}t)$ have a phase difference of 90° , respectively, the general expression of (26) and (27) can be written as

$$c_{\omega_{mod},\phi} = \frac{2}{T} \int_{-T/2}^{T/2} g(t) \cos(\omega_{mod}t + \phi) dt . \quad (28)$$

The magnitude of $c_{\omega_{mod},\phi}$ depends therefore on the frequency ω_{mod} and the phase ϕ . Figure 6 shows a schematic of a lock-in amplifier and links the basic components with Eq. (28).

With the following example we want to illustrate the working principle of a lock-in amplifier. Let us assume a signal $g(t) = \cos(4\omega_{mod}t) + \cos(\omega_{mod}t)$. This signal contains oscillations with the frequencies $4\omega_{mod}$ and ω_{mod} . The lock-in device multiplies internally the signal $g(t)$ with the reference $\cos(\omega_{mod}t)$ resulting in a “combined” signal $h(t) = \cos(4\omega_{mod}t) \cos(\omega_{mod}t) + \cos^2(\omega_{mod}t)$. After integration over one period T of the function $h(t)$ the first term containing the $4\omega_{mod}$ -oscillation vanishes, because positive and negative contributions are equal (see Fig. 7(a)). In contrast, the second term containing the ω_{mod} -oscillation shows a nonzero positive value after integration (see Fig. 7(b)). The lock-in amplifier uses this principle to filter the frequency selected. Additionally, the integrator of the lock-in device integrates over a couple of periods T improving the filter properties [15].

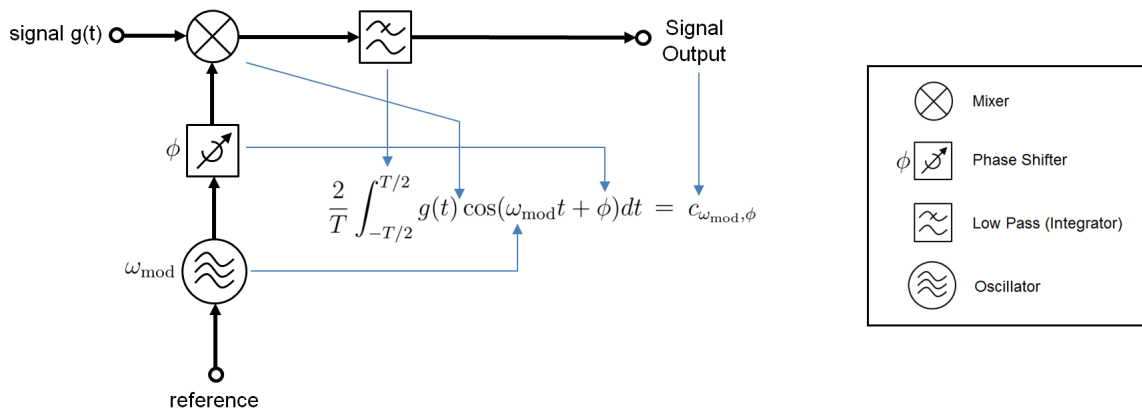


Figure 6: Block diagram of a lock-in amplifier.

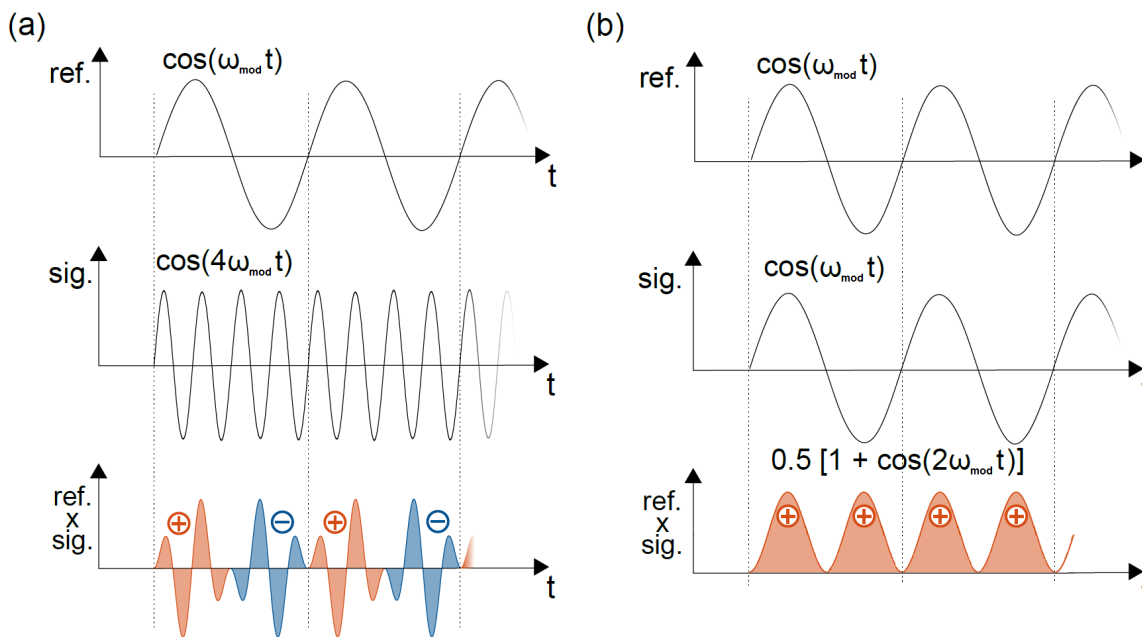


Figure 7: Working principle of a lock-in amplifier. (a) Reference and signal oscillate with different frequencies. The integrated area of the product of signal and reference is equal to zero, because positive and negative contributions cancel each other out. (b) Here the frequency of the signal matches the one of the reference producing a non-zero integrated area of the combined signal.

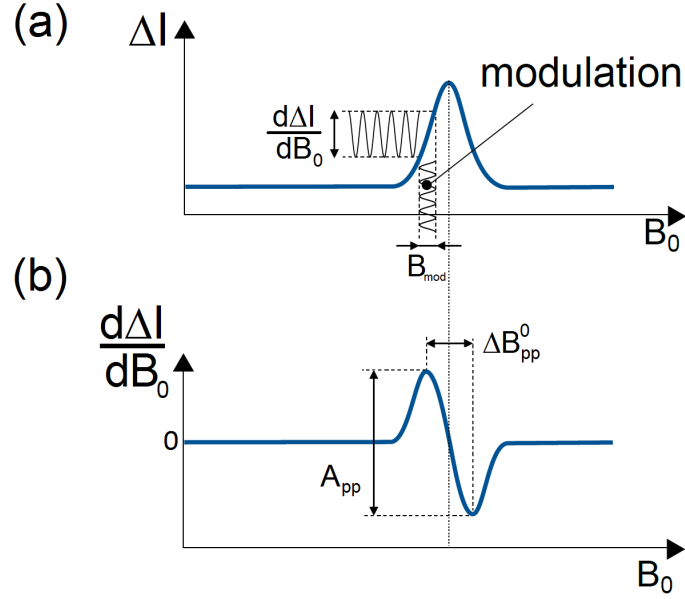


Figure 8: Lock-in detection scheme using magnetic field modulation. (a) Modulating the magnetic field results in a modulated signal $d\Delta I/dB_0$ varying with the modulation frequency and (b) the detected ESR signal becomes the first derivative of the absorption line.

Modulation coils

In the lock-in technique, the magnetic field is modulated in order to perform the phase-sensitive detection at the modulation frequency of the magnetic field, as depicted in Fig. 8(a). Therefore, the detected ESR signal becomes the first derivative of the absorption line $d\Delta I/dB_0$, as shown in Fig. 8(b). The magnetic field modulation is achieved by placing small coils on each side of the resonator. The modulation frequency f_{mod} should be less than the peak-to-peak line width ΔB_{pp}^0 expressed in frequency units,

$$f_{\text{mod}} \ll \frac{g\mu_e}{h} \Delta B_{\text{pp}}^0, \quad (29)$$

in order to avoid a distortion of the line shape. Here, ΔB_{pp}^0 is the line width that would be observed at nearly vanishing amplitude of the magnetic field modulation. When the modulation amplitude B_{mod} is much lower than ΔB_{pp}^0 , the observed line width $\Delta B_{\text{pp}}^{\text{obs}} \approx \Delta B_{\text{pp}}^0$ is unchanged. If the modulation amplitude approaches ΔB_{pp}^0 the observed line begins to broaden and to distort [12]. For $B_{\text{mod}} < \Delta B_{\text{pp}}^0$, the peak-to-peak amplitude A_{pp} of a first derivative line increases linearly with B_{mod} , reaching a maximum for $B_{\text{mod}} \approx 3.5 \Delta B_{\text{pp}}^0$ for Lorentzian-shaped absorption lines [12]. When resolution is important, the modulation amplitude should be at least one-half of the expected structure splitting, provided that the sensitivity is not compromised.

5 Experimental procedure

In this laboratory work, we want to explore the properties of different microwave resonators and understand the working principle of a lock-in detector.

Part I: RLC-Resonator

- (a) To see how the geometry of a resonator affects the resonance frequency, first connect a self-built RLC-resonator to the VNA.
- (b) Calculate the resonance frequency of the resonator by estimating the geometries of coil and capacitor and measure the resonator characteristics with the VNA (S_{11}). Compare the measured resonance frequency with your calculated results.
- (c) Determine the quality factor and the resonance frequency of the RLC-resonator with and without a DPPH sample inside using the VNA. What is the origin of this change?
- (d) Calculate the magnetic field necessary to induce spin flips ($g_e^{\text{DPPH}} = 2.0036$) with your RLC-resonator and drive a magnetic field ramp across this resonance condition measuring S_{11} . Why do we observe an additional shift in resonance frequency and a change of the quality factor when electron spin resonance condition is achieved?

Part II: Cavity Resonator

In this experiment, the cavity resonator allows operation at high frequencies, in this case the resonance frequency is about 9.2 GHz (X-band).

- (a) Repeat the measurement using the same sample (DPPH) as described in Part I (c) and (d) and compare the results obtained from RLC-resonator and the cavity resonator. Why do we obtain a higher quality factor for the cavity resonator when compared to the RLC-resonator?

In order to gain insight into the lock-in working principle, we emulate a lock-in amplifier by setting up the experiment as shown in Fig. 4(b). A modulation unit is employed for both, to apply a modulation field with known frequency f_{mod} and to obtain a time-trace of the S_{11} parameter from which we then filter out the signal modulated with frequency f_{mod} .

- (b) Connect the modulation unit with a frequency of $f_{\text{mod}} \approx 100$ kHz and the VNA to the setup as shown in Fig. 4(b).

- (c) Calculate the required magnetic field for this resonator and drive a magnetic field ramp across the resonance condition to obtain a time-trace signal with the VNA for several modulation periods for each magnetic field point.
- (d) By performing a Fourier analysis as described in Sec. 4 it is possible to extract the desired signal at the modulation frequency f_{mod} or at higher harmonics with high signal-to-noise ratio.
- (e) Compare the results to the measurement without using the lock-in technique recorded in Part II (a).
- (f) To calibrate the magnetic field modulation, investigate the changes of the ESR signal as function of the amplitude of the magnetic field modulation B_{mod} .

Part III: Microstrip Resonator

- (a) Measure the reflection characteristics of the microstrip resonator as a function of the microwave frequency using the VNA and calculate the quality factor.
- (b) Repeat the measurement as described in Part II (c) and (d) using only the lock-in technique.
- (c) Compare the results obtained from Part I, II and III and verify the correlation of resonance frequency and resonance field. What are the advantages of using microstrip resonators in physical metrology?

References

- [1] E. Zavoisky, *Relaxation of liquid solutions for perpendicular fields*, Journal of Physics USSR **9**, 211 (1945)
- [2] A. Abragam and B. Bleaney, *Electron Paramagnetic Resonance of Transition Ions*, Dover Publications, New York (1986)
- [3] G. D. Watkins, *EPR and ENDOR Studies of Defects in Semiconductors*, in M. Stavola (editor), *Identification of Defects in Semiconductors*, volume 51A of *Semiconductors and Semimetals*, Academic Press, San Diego (1998)
- [4] E. R. Cohen and B. N. Taylor, *The 1986 adjustment of the fundamental physical constants*, Review of Modern Physics **59**, 1121 (1987)
- [5] R. M. White, *Quantum Theory of Magnetism*, Springer, Berlin (1983)
- [6] S. Blundell, *Magnetism in Condensed Matter*, Oxford University Press, Oxford (2001)
- [7] A. M. Stoneham, *Theory of Defects in Solids*, Clarendon Press, Oxford (1975)
- [8] M. H. L. Pryce, *A Modified Perturbation Procedure for a Problem in Paramagnetism*, Proceedings of the Physical Society A **63**, 25 (1950)
- [9] F. Bloch, *Nuclear Induction*, Physical Review **70**, 460 (1946)
- [10] G. E. Pake and T. L. Estle, *The Physical Principles of Electron Paramagnetic Resonance*, W. A. Benjamin, London (1973)
- [11] J. A. Weil, J. R. Bolton and J. E. Wertz, *Electron Paramagnetic Resonance: Elementary Theory and Practical Applications*, Wiley, New York (1994)
- [12] C. P. Poole, *Electron Paramagnetic Resonance: A Comprehensive Treatise on Experimental Techniques*, Dover Publications, Mineola (1997)
- [13] W. Demtröder, *Experimentalphysik 2: Elektrizität und Optik*, Springer, Berlin (2008)
- [14] R. Narkowicz, D. Suter and R. Stonies, *Planar microresonators for EPR experiments*, J. Magn. Reson. **175**, 275 (2005)
- [15] *Manual of Lock-In Amplifier SR380*, Stanford Research Systems

Acknowledgements

This Fortgeschrittenenpraktikumsversuch was partly funded by Studienbeiträge 2011/2012. The microstrip resonator has been provided by Prof. Suter from Universität Dortmund.